Balanced Splitting and Rebalanced Splitting

Citation: Speth, Raymond L., William H. Green, Shev MacNamara, and Gilbert Strang. "Balanced Splitting and Rebalanced Splitting." SIAM Journal on Numerical Analysis 51, no. 6 (January 2013): 3084–3105. © 2013, Society for Industrial and Applied Mathematics

As Published: http://dx.doi.org/10.1137/120878641

Publisher: Society for Industrial and Applied Mathematics

Persistent URL: http://hdl.handle.net/1721.1/86001

Version: Final published version: final published article, as it appeared in a journal, conference proceedings, or other formally published context

SIAM J. NUMER. ANAL.
Vol. 51, No. 6, pp. 3084–3105

BALANCED SPLITTING AND REBALANCED SPLITTING*

RAYMOND L. SPETH†, WILLIAM H. GREEN†, SHEV MACNAMARA‡, AND GILBERT STRANG‡

Abstract. Many systems of equations fit naturally in the form $du/dt = A(u) + B(u)$. We may separate convection from diffusion, x-derivatives from y-derivatives, and (especially) linear from nonlinear. We alternate between integrating operators for $dv/dt = A(v)$ and $dw/dt = B(w)$. Noncommutativity (in the simplest case, of e^{Ah} and e^{Bh}) introduces a splitting error which persists even in the steady state. Second-order accuracy can be obtained by placing the step for B between two half-steps of A. This splitting method is popular, and we suggest a possible improvement, especially for problems that converge to a steady state. Our idea is to adjust the splitting at each timestep to $[A(u) + c_n] + [B(u) - c_n]$. We introduce two methods, balanced splitting and rebalanced splitting, for choosing the constant c_n. The execution of these methods is straightforward, but the stability analysis becomes more difficult than for $c_n = 0$. Experiments with the proposed rebalanced splitting method indicate that it is much more accurate than conventional splitting methods as systems approach steady state. This should be useful in large-scale simulations (e.g., reacting flows). Further exploration may suggest other choices for c_n which work well for different problems.

Key words. Strang splitting, steady state, advection–diffusion, reaction, combustion

AMS subject classifications. 35K57, 65M12, 65M20, 80A25

DOI. 10.1137/120878641

1. Introduction.

Suppose a system of differential equations contains terms with disparate approximations. Our prime example is reacting flow with N species. The evolution of the mass fractions $Y_1, \ldots, Y_N$ is governed by convection, diffusion, and reaction:

$$\frac{\partial Y_k}{\partial t} = -\mathbf{v} \cdot \nabla Y_k + D_k \nabla^2 Y_k + r_k(Y_1, \ldots, Y_N). \tag{1.1}$$

The prescribed velocity field is $\mathbf{v}(\mathbf{r})$, D_k is the diffusion coefficient of species k, and r_k is the net rate at which species k is produced. Spatial discretization of the advection and diffusion terms leads to difference matrices in which neighboring mesh points are coupled, but each species is independent. On the other hand, the reaction term is local in space, but couples all the species together. The reaction term is almost always nonlinear and usually makes the PDE system (1.1) very stiff.

Because the approximations for these terms are so different, it is natural to consider *splitting methods* [8, 23, 26, 29]. Each term can be integrated using methods which take advantage of its special structure. To avoid stability problems, the transport terms are sometimes treated implicitly, requiring an efficient linear solver. Splitting methods themselves may introduce stability issues as well [27]. Integration of the reaction terms (which is usually the most computationally intensive, since N is often

*Received by the editors May 25, 2012; accepted for publication (in revised form) August 5, 2013; published electronically November 19, 2013.

http://www.siam.org/journals/sinum/51-6/87864.html

†Chemical Engineering, MIT, Cambridge, MA 02139 (speth@mit.edu, whgreen@mit.edu). The first author was partly supported by the US Department of Energy (Office of Basic Energy Sciences, Division of Chemical Sciences, Geosciences, and Biosciences) under contract DE-FG02-98ER14914.

‡Mathematics, MIT, Cambridge, MA 02139 (shev.mac@gmail.com, gs@math.mit.edu). The third author received a Fulbright Scholarship and an MIT Energy Initiative Fellowship. The fourth author was supported by NSF grant 1023152 and the Mathworks Professorship at MIT.

large and the equations are very stiff) can be done in parallel, since each mesh point is independent.

Begin with a system where both parts of the equation are linear:

$$\frac{dy}{dt} = (Ay + a) + (By + b). \tag{1.2}$$

The exact solution to this equation with matrices A and B is

$$y(t) = y_\infty + e^{(A+B)t}\big(y(0) - y_\infty\big), \tag{1.3}$$

where the steady-state solution y_∞ is given by

$$(A + B)y_\infty = -(a + b). \tag{1.4}$$

If this is treated using splitting, the substeps will surely involve approximations to the one-step exponentials e^{Ah} and e^{Bh}. If we take an exact e^{Ah} substep and then an e^{Bh} substep, the error in the overall step involves the difference between $e^{Bh}e^{Ah}$ and $e^{(A+B)h}$. In general these differ by $\mathcal{O}(h^2)$ over each step of size h:

$$\begin{aligned} e^{Bh}e^{Ah} &= \left(I + Bh + \frac{1}{2}B^2h^2 + \cdots\right)\left(I + Ah + \frac{1}{2}A^2h^2 + \cdots\right) \\ &= I + (A + B)h + \frac{1}{2}(A^2 + B^2 + 2BA)h^2 + \cdots \\ &= e^{(A+B)h} + \frac{1}{2}(BA - AB)h^2 + \cdots . \end{aligned} \tag{1.5}$$

The commutator $[B, A] = BA - AB$ is nonzero in most practical problems, so this splitting is only *first-order accurate*. The $\mathcal{O}(h^2)$ errors at every step combine into an $\mathcal{O}(h)$ overall error after $\mathcal{O}(1/h)$ steps.

Another way to analyze the accuracy of splitting methods is to let $e^C = e^Ae^B$, where $C(A, B) \equiv A + B + \frac{1}{2}[A, B] + \cdots$ is the Baker–Campbell–Hausdorff (BCH) formula in which higher-order terms involve nested commutators. A type of BCH formula for second-order splitting (introduced below) could come from applying the known formula twice to get $C(Ah/2, C(Bh, Ah/2))$ [32, 11].

An improvement to achieve second-order accuracy was suggested in [29] by "symmetrizing" the overall step. We see the crucial matrix most clearly when $a = b = 0$:

$$\textit{Second-order splitting} \qquad y(h) = e^{Ah/2}e^{Bh}e^{Ah/2}y(0). \tag{1.6}$$

This approach captures the correct $\frac{1}{2}(A + B)^2h^2$ term in the exponential, but it has an error in the h^3 term:

$$e^{Ah/2}e^{Bh}e^{Ah/2} - e^{(A+B)h} = \frac{1}{24}\left([[A, B], A] + 2[[A, B], B]\right)h^3 + \mathcal{O}(h^4). \tag{1.7}$$

Other authors have undertaken the serious work of developing that idea into full-scale codes (reacting flow problems in combustion [28] are important examples). The extra cost of replacing one full step by three substeps has been found acceptable, since it allows one to take advantage of the partial decoupling discussed above.

For simplicity we have described splitting as if the substeps use exact exponentials. In practice $e^{Ah/2}$ and e^{Bh} are replaced by applying numerical integration schemes such

as Runge–Kutta or backward differences sequentially to the split equations:

$$\frac{dz_1}{dt} = Az_1 + a; \quad z_1(t) = y(t), \tag{1.8}$$

$$\frac{dz_2}{dt} = Bz_2 + b; \quad z_2(t) = z_1(t + h/2), \tag{1.9}$$

$$\frac{dz_3}{dt} = Az_3 + a; \quad z_3(t + h/2) = z_2(t + h), \tag{1.10}$$

$$y(t + h) = z_3(t + h). \tag{1.11}$$

Second-order splitting (sometimes called Strang splitting) is used in a wide range of applications.

We would like to add two comments from the existing literature before we introduce balanced splitting. First, it is natural to ask about third-order accuracy (or higher). This is only possible by allowing substeps that go backward in time or forward in "complex time" [2, 32, 11, 17]. For diffusion equations, backward timesteps introduce unacceptable numerical instabilities. A complex $\Delta t_1 = a + ib$ followed by $\Delta t_2 = a - ib$ is, in theory, possible, but not often chosen. For reaction–diffusion equations second-order accuracy may be best possible in practice.

Second, in nonlinear problems we want approximations that are *symplectic*. Then area in phase space is conserved, and approximate solutions to nearby problems remain close. The beautiful book of Hairer, Lubich, and Wanner [11, pp. 47, 230] confirms that second-order splitting (modeled by $e^{Ah/2}e^{Bh}e^{Ah/2}$ in linear problems) is truly symplectic for nonlinear equations.

2. Steady-state solutions. Splitting in time-dependent problems has led to algorithms for the solution of a related problem: *capture the steady state*. Each timestep becomes an iteration toward a solution y_∞ that is independent of time. Then dy/dt is removed from the equation, leaving a balance between the time-independent terms. For the reacting flow problem in section 9, the transport and reaction terms balance to produce a steady flame. For reaction-diffusion systems, steady state may be a visually interesting pattern [19].

In this approach to y_∞, splitting methods may produce *different* steady-state solutions from the original ODE system. Consider as an example the nonlinear, inhomogeneous equation

$$y' = (y + 2) - \frac{1}{4}y^4 \tag{2.1}$$

with the initial condition $y(0) = 0.5$ and the steady solution $y_\infty = 2$. In Figure 2.1(a), we demonstrate the first-order sequential splitting process as applied to (2.1) using a timestep of $h = 0.5$. The split terms follow trajectories that are quite different from the solution to the original equation. Even when the splitting method has reached its steady state, $y_\infty \approx 1.36$ for $h = 0.5$, the individual steps take the solution away from y_∞ before returning. Decreasing the timestep to $h = 0.1$ decreases the steady-state error ($y_\infty \approx 1.82$ in Figure 2.1(b)). However, arbitrarily small timesteps are required to effectively eliminate the steady-state error even when the solution is slowly varying.

Figures 2.1(c) and 2.1(d) show the second-order (Strang) splitting process applied to the same problem. While the substep deviations within each combined step remain large, the error in y_∞ is significantly smaller ($y_\infty \approx 2.31$ for $h = 0.5$ and $y_\infty \approx 2.01$ for $h = 0.1$). The goal of balanced splitting is to reduce or remove this steady-state error.

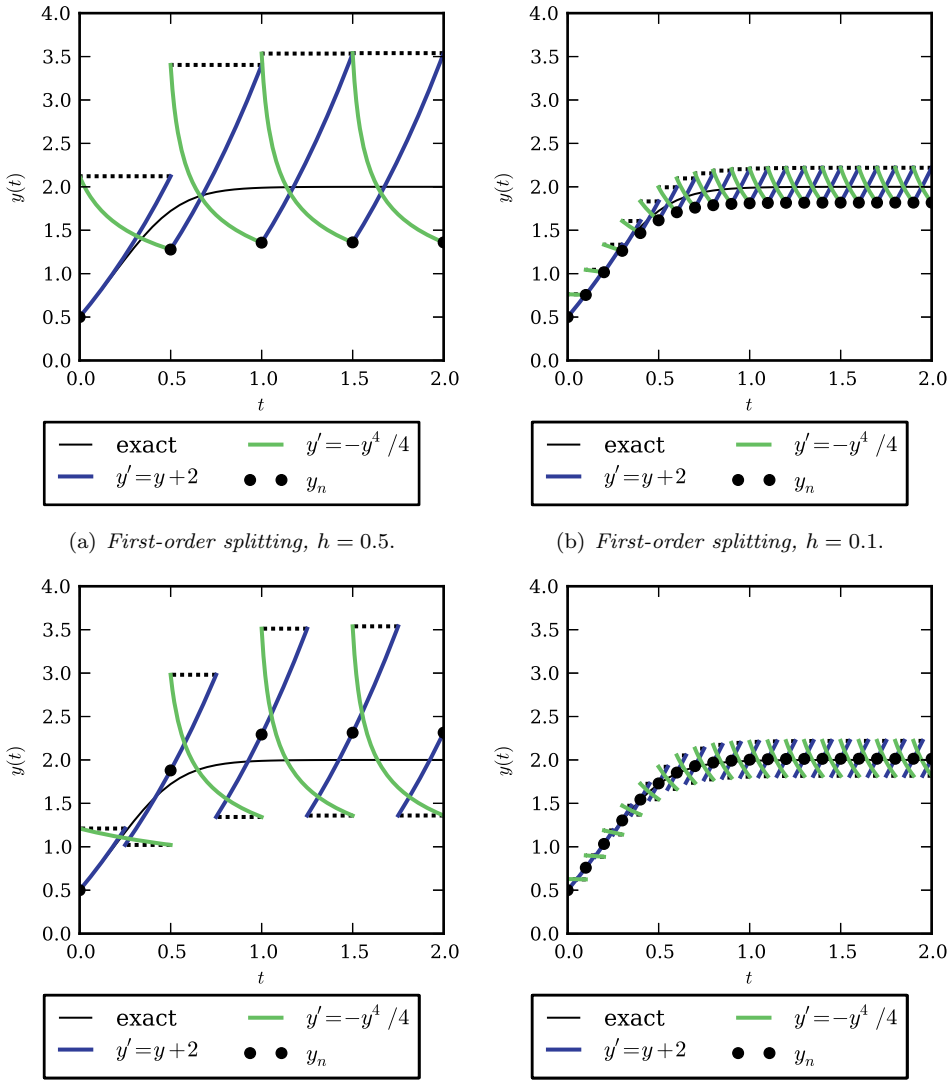

(a) *First-order splitting,* $h = 0.5$.

(b) *First-order splitting,* $h = 0.1$.

(c) *Second-order splitting,* $h = 0.5$.

(d) *Second-order splitting,* $h = 0.1$.

FIG. 2.1. *First-order splitting* (a, b) *and second-order splitting* (c, d) *applied to* (2.1). *See Figure* 5.1(b) *for further improvement from balancing.*

For a more general analysis, consider again the inhomogeneous linear model problem (1.2). The steady-state equation is

$$(Ay_\infty + a) + (By_\infty + b) = 0. \tag{2.2}$$

If $A + B$ is a stable matrix (its eigenvalues have negative real parts), then the time-dependent solution of the differential equations converges to y_∞:

$$y_\infty = -(A + B)^{-1}(a + b). \tag{2.3}$$

We will discuss below the stability of splitting methods. Certainly if A and B are symmetric negative definite, and the step size h is small, reasonable methods converge

safely to $y_\infty = 0$ in the simplest case $a = b = 0$. *Do we get the correct steady state y_∞ in the general case, linear or nonlinear?* The answer is *no*. It is very possible that y_∞ is not a steady state for the separate substeps.

It is worth noting the special cases under which splitting does preserve the steady state. If $A^{-1}a = B^{-1}b$, then each half of (1.2) independently satisfies the steady state, i.e., $Ay_\infty + a = 0$ and $By_\infty + b = 0$. Such special cases are uncommon, outside the homogeneous case where $a = b = 0$. Additionally, if the commutator $[A, B] = 0$ (which holds if and only if $e^{h(A+B)} = e^{hA}e^{hB}$ for all h), splitting is exact. These conditions are further discussed in section 8.

In general, our previous comparison of Taylor series expansions shows that, at steady state, first-order splitting introduces a nonzero error $(e^{h(A+B)} - e^{Bh}e^{Ah})y_\infty \approx \frac{1}{2}h^2[B, A]y_\infty$. Naively, this suggests that the error at the steady state is approximately $\mathcal{O}(h^2)$. However, this assumes that we start at the exact steady state y_∞ and take only one split timestep. It is more realistic to start with an arbitrary initial condition and integrate until we reach the split solver's steady state z_∞. In general the error $z_\infty - y_\infty$ is approximately $\mathcal{O}(h)$ for first-order splitting. For Strang splitting, the error $z_\infty - y_\infty$ is approximately $\mathcal{O}(h^2)$ (see Appendix A).

3. Strong stability. Strong stability is present when the norm of the solution to $u' = Au$ is monotone decreasing for all initial values $u(0)$:

$$||u(t)|| = ||e^{At}u(0)|| \le ||u(0)||. \tag{3.1}$$

Equivalently $||e^{At}|| \le 1$ for $t \ge 0$. This is more restrictive than stability of the eigenvalues of A: $Re\{\lambda(A)\} \le 0$. For simple eigenvalues, negative real parts only ensure that e^{At} is bounded. Multiple eigenvalues allow polynomial growth $||e^{At}|| < C(1 + t^k)$. These eigenvalue conditions might hold separately for A and B, but not for their sum $A + B$ (this is Turing instability and the opposite can also hold). In the absence of symmetry, eigenvalues give only limited control.

We note here a familiar fact, that the *symmetric part* of A governs strong stability.

LEMMA 3.1. *Strong stability* (3.1) *holds if and only if $A + A^*$ is negative definite or semidefinite (where A^* is the conjugate transpose of A).*

Proof. The simplest approach computes the derivative of $||u(t)||^2$:

$$\begin{aligned} \frac{d}{dt}(u(t), u(t)) &= (u'(t), u(t)) + (u(t), u'(t)) \\ &= (Au(t), u(t)) + (u(t), Au(t)) \\ &= ((A + A^*)u(t), u(t)). \end{aligned} \tag{3.2}$$

This is never positive (and $||u(t)||^2$ is never increasing) exactly when $A + A^*$ is negative semidefinite. ∎

When strong stability holds separately for A and B, it follows immediately that first-order and second-order splitting are also strongly stable:

$$||e^{Bh}e^{Ah}|| \le 1 \qquad \text{and} \qquad ||e^{Ah/2}e^{Bh}e^{Ah/2}|| \le 1. \tag{3.3}$$

We will not have complete control over balanced splitting, but in our experience we can achieve stability there, too.

Example. Before reaction terms are introduced, consider a one-dimensional, scalar advection–diffusion equation:

$$u_t = -au_x + bu_{xx}, \tag{3.4}$$

which we wish to approximate as a system of ODEs:

$$u' = Cu + Du. \tag{3.5}$$

Suppose that splitting separates advection $-au_x$ from diffusion bu_{xx}. Diffusion is represented by a negative definite second difference matrix D such as

$$D = \frac{b}{h^2}\begin{bmatrix} -2 & 1 & & \\ 1 & -2 & 1 & \\ & \ddots & \ddots & \ddots \end{bmatrix}, \quad \text{with } D + D^T < 0.$$

The first and last rows depend on the boundary conditions. Advection is represented by a first difference matrix, possibly centered and antisymmetric:

$$C \approx -a\Delta_0 = \frac{a}{2h}\begin{bmatrix} 0 & -1 & & \\ 1 & 0 & -1 & \\ & \ddots & \ddots & \ddots \end{bmatrix}, \quad \text{with } \Delta_0 + \Delta_0^T = 0.$$

The combination is strongly stable. It may be more instructive to consider one-sided differences, where advection is represented by

$$C = C_+ = -a\Delta_+ = \frac{a}{h}\begin{bmatrix} 1 & -1 & & \\ & 1 & -1 & \\ & & \ddots & \ddots \end{bmatrix} \tag{3.6}$$

or

$$C = C_- = -a\Delta_- = \frac{a}{h}\begin{bmatrix} -1 & & & \\ 1 & -1 & & \\ & 1 & -1 & \\ & & \ddots & \ddots \end{bmatrix}. \tag{3.7}$$

One of these is *upwind* and the other is *downwind*, depending on the sign of a (which gives the direction of the flow). Pure advection, $u_t = -au_x$, would be solved by a function of $x - at$. If $a > 0$, Δ_- is the appropriate choice because the derivative at a point x depends on points *upwind* of x. We see this in the negative definiteness of the symmetric part, which differs from the second difference matrix D only by a constant factor:

$$C_- + C_-^T = \frac{ha}{b}D. \tag{3.8}$$

The centered difference Δ_0 has greater accuracy and is the natural choice. But when $|a|$ is large (and advection dominates diffusion), Δ_0 can be numerically dangerous. This matrix can be nearly singular and Δ_- might be better. Advection–diffusion–reaction problems are discussed by many authors (see [13] or [28]) and perhaps no comprehensive solution has been found.

Given a strongly stable differential equation $u' = Au$, finite difference stability can become harder to maintain in two limiting cases:

1. The real parts of $\lambda(A)$ become large and negative.
2. The imaginary parts of $\lambda(A)$ become large.

And for systems, two more difficulties can enter when the coefficients are matrices:

3. (stiff systems) Two negative eigenvalues can produce decay at very different time scales: $|\lambda_2| \gg |\lambda_1|$.
4. A and B can fail to commute. For ordinary splitting and strong stability we can appeal to (3.3).

We will see that balanced splitting reconnects A and B, making stability harder to analyze but usually improving the computed steady state.

4. Balanced splitting. The goal of this paper is the development of a stable second-order method that correctly balances the substeps. By moving a constant vector between the two parts, we can assure *the same steady state for each part.* This becomes a suitable steady state for the whole timestep.

Consider a system of nonlinear differential equations, with two parts that might be transport and reaction terms $\mathcal{T}(y)$ and $\mathcal{R}(y)$:

$$\textit{time-dependent} \qquad y' = \mathcal{T}(y) + \mathcal{R}(y), \tag{4.1}$$

$$\textit{steady state} \qquad 0 = \mathcal{T}(y_\infty) + \mathcal{R}(y_\infty). \tag{4.2}$$

The idea of balanced splitting is to move a constant vector from one part to the other (before each timestep). If we were at steady state, $y = y_\infty$, the vector to move would be $c_\infty = \frac{1}{2}(\,\mathcal{R}(y_\infty) - \mathcal{T}(y_\infty)\,)$. This offset means that the parts $\mathcal{T}^* = \mathcal{T} + c$ and $\mathcal{R}^* = \mathcal{R} - c$ have the correct steady-state solution from (4.2):

$$\mathcal{T}^*(y) = \mathcal{T}(y) + \frac{1}{2}(\,\mathcal{R}(y_\infty) - \mathcal{T}(y_\infty)\,) = 0 \text{ at } y = y_\infty,$$

$$\mathcal{R}^*(y) = \mathcal{R}(y) - \frac{1}{2}(\,\mathcal{R}(y_\infty) - \mathcal{T}(y_\infty)\,) = 0 \text{ at } y = y_\infty.$$

Balanced splitting comprises a family of methods with different procedures for determining the balancing constant c_n for each timestep such that the steady state for the whole system is an approximate steady state for each of the two parts.

We now describe and analyze two such methods: "Simple balanced splitting" is the first approach. Its stability will be seen to depend on the ratio A/B, which is not acceptable even in the scalar case. "Rebalanced splitting" uses earlier values (and substep values) for greatly improved stability.

Exploring other choices for the balancing constant may be worthwhile as well. We describe these splitting methods in the nonlinear case, and then discuss stability for the linear model problem $y' = (Ay + a) + (By + b)$.

In the linear case, balanced splitting becomes identical with the usual Strang splitting for an augmented system with one additional unknown:

$$\frac{d}{dt}\begin{bmatrix} y \\ z \end{bmatrix} = \begin{bmatrix} A & a+c \\ 0 & 0 \end{bmatrix}\begin{bmatrix} y \\ z \end{bmatrix} + \begin{bmatrix} B & b-c \\ 0 & 0 \end{bmatrix}\begin{bmatrix} y \\ z \end{bmatrix}. \tag{4.3}$$

Setting $z = 1$ and $c = 0$ gives ordinary splitting (with no balancing) for the model problem with nonzero a and b. The splitting is exact when $\hat{A}\hat{B} = \hat{B}\hat{A}$ ($\hat{A}$ includes the extra column vector $a+c$ and the row of zeros, and similarly for $\hat{B}$). This is equivalent to $[A, B] = 0$ and $A^{-1}a = B^{-1}b = 0$.

This approach confirms that balanced splitting has second-order accuracy for any choice of the balancing constant vector c.

5. Simple balanced splitting. Since y_∞ is not known, we create a new balancing vector c_n at each step from the current values of the approximate solution y_n. The most straightforward choice is

$$\text{(5.1)} \qquad \textit{Simple balanced splitting} \qquad c_n = \frac{1}{2}\big(\mathcal{R}(y_n) - \mathcal{T}(y_n)\big).$$

At each step we compute c_n and solve (approximately, from t_n to t_{n+1}) the equation with balanced parts:

$$\text{(5.2)} \qquad y' = \mathcal{T}_n^*(y) + \mathcal{R}_n^*(y) = \big(\mathcal{T}(y) + c_n\big) + \big(\mathcal{R}(y) - c_n\big).$$

That step starts from y_n and produces y_{n+1}. The integration proceeds accordingly:

$$\text{(5.3)} \qquad \frac{dz_1}{dt} = \mathcal{T}(z_1) + c_n; \quad z_1(t_n) = y_n,$$

$$\text{(5.4)} \qquad \frac{dz_2}{dt} = \mathcal{R}(z_2) - c_n; \quad z_2(t_n) = z_1(t_n + h/2),$$

$$\text{(5.5)} \qquad \frac{dz_3}{dt} = \mathcal{T}(z_3) + c_n; \quad z_3(t_n + h/2) = z_2(t_n + h),$$

$$\text{(5.6)} \qquad y_{n+1} = z_3(t_n + h).$$

Then (5.1) yields the offset c_{n+1} to apply in the following timestep.

To illustrate, we apply simple balanced splitting to the previously introduced scalar nonlinear problem (2.1). In Figures 5.1(a) and 5.1(b) the step sizes are again $h = 0.5$ and $h = 0.1$. Even with the large step size, the solution quickly converges to the true steady state, with an error at $t = 2.0$ of $\Delta y = 2.2 \times 10^{-2}$ for the larger timestep and $\Delta y = 6.5 \times 10^{-6}$ for the smaller step. Furthermore, the trajectories followed by the individual integration steps remain close to the exact solution.

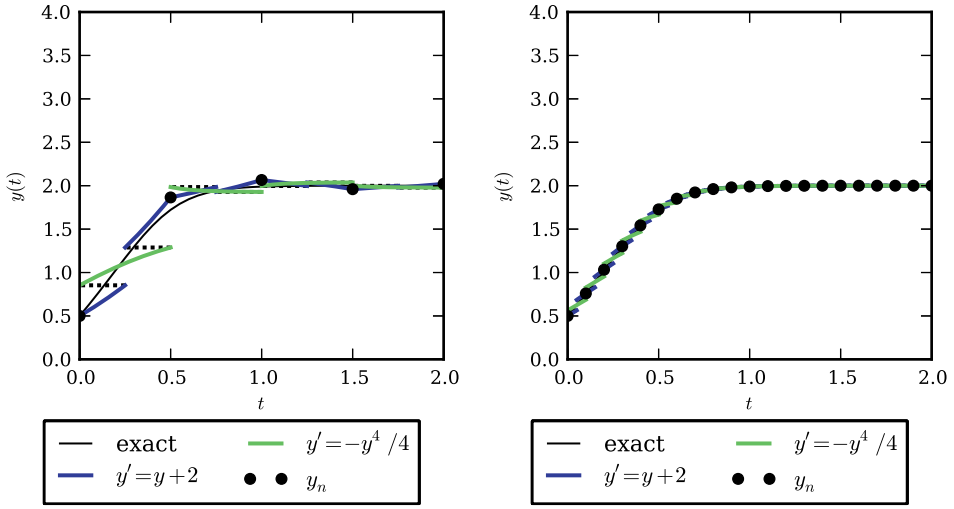

(a) *Simple balanced splitting,* $h = 0.5$. (b) *Simple balanced splitting,* $h = 0.1$.

FIG. 5.1. *Simple balanced splitting applied to* (2.1). *Note the error reduction when compared with the solutions obtained using conventional splitting methods shown in Figure* 2.1.

6. Linear analysis of simple balanced splitting. In the linear model with constant coefficient matrices A and B, this simple balanced splitting becomes

$$y' = (Ay + a + c_n) + (By + b - c_n) \quad \text{with}$$
$$c_n = \frac{1}{2}\big[(By_n + b) - (Ay_n + a)\big]. \tag{6.1}$$

Suppose we apply the second-order "Strang splitting" and assume *exact integration* over each substep. For convenience, let us adopt the following notation:

$$\alpha = e^{Ah/2}, \quad \beta = e^{Bh}, \quad A^* = (\alpha - I)A^{-1}, \quad B^* = (\beta - I)B^{-1}. \tag{6.2}$$

The first half-step starts at y_n and reaches y_n^+ by integrating $y' = Ay + a + c_n$:

$$y_n^+ = \alpha y_n + A^*(a + c_n). \tag{6.3}$$

Starting from y_n^+ the next substep integrates $y' = By + b - c_n$ to reach y_n^{++}:

$$y_n^{++} = \beta\alpha y_n + \beta A^*(a + c_n) + B^*\,(b - c_n)\,. \tag{6.4}$$

The third substep integrates $y' = Ay + a + c_n$ starting from y_n^{++}:

$$y_{n+1} = \alpha\beta\alpha y_n + \alpha B^*(b - c_n) + (\alpha\beta + I)\,A^*(a + c_n). \tag{6.5}$$

To study the stability (or instability) of this iteration, substitute c_n from (6.1) into (6.5). The result is a recurrence relation that yields y_{n+1} from y_n:

$$y_{n+1} = Ry_n + Q(a + b). \tag{6.6}$$

The growth factor R controls this recursion:

$$R = \alpha\beta\alpha + \frac{1}{2}\big[\alpha B^* - (\alpha\beta + I)A^*\big](A - B). \tag{6.7}$$

The matrix factor Q for the inhomogeneous term is

$$Q = \frac{1}{2}\big[\alpha B^* + (\alpha\beta + I)A^*\big]. \tag{6.8}$$

The factors R and Q may be compared to the corresponding terms appearing in the exact solution:

$$(y_{n+1})_{\text{exact}} = e^{(A+B)h}y_n + \Big(e^{(A+B)h} - I\Big)\,(A + B)^{-1}(a + b). \tag{6.9}$$

The first term in R comes from normal "Strang splitting" and the second term comes from balancing. The balancing term is $\mathcal{O}(h^3)$ and the first term is $e^{(A+B)h} + \mathcal{O}(h^3)$. Q may be rewritten as

$$(\alpha\beta\alpha - I)(A + B)^{-1} + \frac{1}{2}\left[\alpha(\beta - I)\left(B^{-1} + A^{-1}\right) - (\alpha\beta\alpha - I)A^{-1}\right](A - B)(A + B)^{-1}. \tag{6.10}$$

The first term is $(e^{(A+B)h} - I)(A+B)^{-1} + \mathcal{O}(h^3)$ and the second term is $\mathcal{O}(h^3)$. Thus second-order accuracy is confirmed.

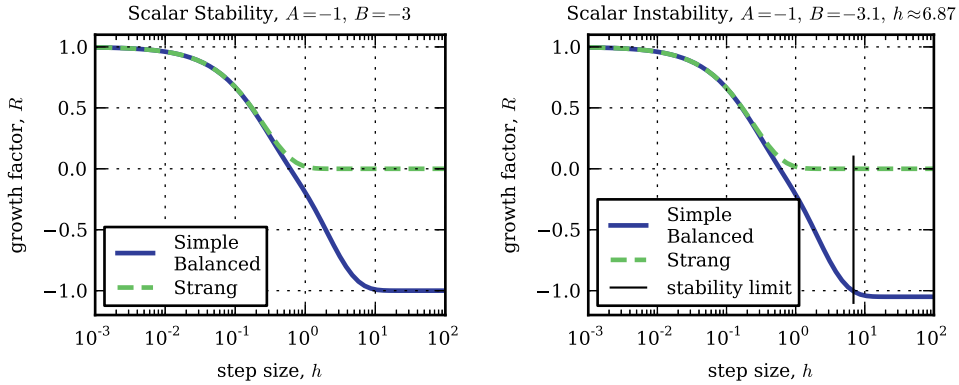

FIG. 6.1. *In the scalar case, Strang splitting is exact. Left:* $|B| = 3|A|$ *and simple balanced splitting is stable. Right:* $|B| > 3|A|$, *and* $R < -1$ *for large* h. *The vertical line marks the approximation* (6.14) *to the maximum step size allowable before instability.*

The balanced splitting method is especially accurate as the system approaches steady state. The correct steady state of the original problem, $y_\infty = -(A+B)^{-1}(a+b)$, satisfies the balanced splitting recursion relation (6.6) for all values of h. In contrast, unbalanced ($c_n = 0$) Strang splitting has the h-dependent steady state:

$$z_\infty = (I - \alpha\beta\alpha)^{-1}\big[\alpha B^* b + (\alpha\beta + I)A^* a\big]. \tag{6.11}$$

This method of simple balancing is stable if all eigenvalues of the growth factor R have $|\lambda| < 1$. It is instructive to consider the limiting value of R as $h \to \infty$. We assume that the eigenvalues of both A and B have negative real parts (stability for each part in the splitting). Then both α and β approach zero, so that

$$\lim_{h\to\infty} R = \frac{1}{2}A^{-1}(A - B) = \frac{1}{2}(I - A^{-1}B). \tag{6.12}$$

In the scalar case, the test $|R| < 1$ says that stability for large h depends on the ratio B/A of negative numbers. *If that ratio exceeds* 3, then the limiting value of R is below $\frac{1}{2}(1-3) = -1$. *Simple balancing is unstable for large* h, when $|B| > 3|A|$.

The plot of R shows stability (scalar case only!) for $B = 3A$ (Figure 6.1). There is instability for $h > 7$ when $B/A = 3.1$ (and for $h > 0.7$ when $B/A = 10$).

LEMMA 6.1. *A sufficient condition for scalar stability is* $A < B < 0$.

Proof. Write (6.7) as the sum $R = (R_1 + R_2 + R_3)/2$, where

$$\begin{aligned} R_1 &= I - A^{-1}B + \alpha\beta\alpha(I + A^{-1}B), \\ R_2 &= \alpha(\beta - I)B^{-1}A, \\ R_3 &= -\alpha(\beta - I)A^{-1}B. \end{aligned} \tag{6.13}$$

Given $A < B < 0 < h$, then $0 < \alpha\beta\alpha < 1$ and $0 < A^{-1}B < 1$. This yields $0 < R_1 < 2$.

Clearly R_2 is negative and R_3 is positive. Their sum $R_2 + R_3$ is negative because $B^{-1}A > A^{-1}B$. We want a lower bound on R_2:

$$R_2 = [hA\alpha]\left[(\beta - I)/hB\right] = \left[hAe^{hA/2}\right]\left[\left(e^{hB} - I\right)/hB\right].$$

The first factor is most negative at $hA = -2$, where it equals $-2/e$. The second factor never exceeds 1 for $hB < 0$. So R_2 is not smaller than $-2/e$ and

$$R = \frac{1}{2}(R_1 + R_2 + R_3) \le \frac{1}{2}R_1 < 1,$$
$$R = \frac{1}{2}(R_1 + R_2 + R_3) > \frac{1}{2}R_2 \ge -\frac{1}{e}.$$

Thus simple balanced splitting (scalar case) has $|R| < 1$ for all $h > 0$ if $A < B < 0$. □

Numerical examples in Figure 6.1 suggest that the stability condition may be relaxed to $3A < B < 0$. Further, heuristic analysis suggests *an explicit approximation to the maximum step size allowable*:

$$h \approx \frac{2}{A} \ln\left(1 - 3\frac{A}{B}\right). \tag{6.14}$$

Figure 6.1 shows an example where this approximation is very accurate. For the case where $A = -1, B = -3.1$, shown in the figure, the heuristic predicts the maximum allowable step size to be $h \approx 6.87$, which is close to the exact stability limit of $h \approx 6.65$ found by solving (6.7) with $R = -1$.

7. Rebalanced splitting. We now construct a more stable scheme, in which the balancing vector c involves the intermediate values y^+ and y^{++} from the previous split step (as well as the old and new values of y). Remember from (5.1) that c has the form $\frac{1}{2}(\mathcal{R}^{**} - \mathcal{T}^{**})$, where $\mathcal{R}^{**}$ and $\mathcal{T}^{**}$ are approximations for $\mathcal{R}(y)$ and $\mathcal{T}(y)$, respectively. Then the transport–reaction splitting in (5.2) is balanced:

$$y' = \mathcal{T}_n^*(y) + \mathcal{R}_n^*(y) = \big(\mathcal{T}(y) + c_n\big) + \big(\mathcal{R}(y) - c_n\big). \tag{7.1}$$

The split integration steps give the intermediate values y_n^+ and y_n^{++}:

$$y_n^+ = y_n + \int_{t_n}^{t_n + h/2} \big(\mathcal{T}(y) + c_n\big)\, dt, \tag{7.2}$$

$$y_n^{++} = y_n^+ + \int_{t_n}^{t_n + h} \big(\mathcal{R}(y) - c_n\big)\, dt, \tag{7.3}$$

$$y_{n+1} = y_n^{++} + \int_{t_n + h/2}^{t_n + h} \big(\mathcal{T}(y) + c_n\big)\, dt. \tag{7.4}$$

In rebalanced splitting, we use average values of $\mathcal{T}(y)$ and $\mathcal{R}(y)$ over the previous timestep to compute $\mathcal{R}^{**}$ and $\mathcal{T}^{**}$:

$$\mathcal{T}_{n+1}^{**} = \frac{1}{h}\int_{t_n}^{t_n + h} \mathcal{T}(y)\, dt = \frac{(y_{n+1} - y_n^{++}) + (y_n^+ - y_n)}{h} - c_n, \tag{7.5}$$

$$\mathcal{R}_{n+1}^{**} = \frac{1}{h}\int_{t_n}^{t_n + h} \mathcal{R}(y)\, dt = \frac{y_n^{++} - y_n^+}{h} + c_n. \tag{7.6}$$

Then c_{n+1} comes from this new "rebalanced" formula:

$$c_{n+1} = \frac{1}{2h}\left(-y_{n+1} + 2y_n^{++} - 2y_n^+ + y_n\right) + c_n. \tag{7.7}$$

8. Linear analysis of rebalanced splitting. We continue with the linear inhomogeneous system

$$y' = (Ay + a + c) + (By + b - c). \tag{8.1}$$

With $c = c_n$ the intermediate and final values y_n^+, y_n^{++}, y_{n+1} come from a step of the usual Strang splitting. Equations (6.3)–(6.5) still apply but now (7.7) produces a new expression for c_{n+1}:

$$c_{n+1} = Uy_n + Vc_n + S \tag{8.2}$$

with matrix coefficients U, V and the vector S:

$$\begin{aligned} U &= \frac{1}{2h}(-\alpha\beta\alpha + 2\beta\alpha - 2\alpha + I), \\ V &= \frac{1}{2h}\big[(-\alpha\beta + 2\beta - 3I)A^* + (\alpha - 2I)B^* + 2hI\big], \\ S &= \frac{1}{2h}\big[(-\alpha\beta + 2\beta - 3I)A^*a - (\alpha - 2I)B^*b\big]. \end{aligned}$$

Equation (6.5) for y_{n+1} combines with (8.2) to produce a vector recurrence:

$$\begin{bmatrix} y_{n+1} \\ c_{n+1} \end{bmatrix} = \begin{bmatrix} P & Q \\ U & V \end{bmatrix} \begin{bmatrix} y_n \\ c_n \end{bmatrix} + \begin{bmatrix} R \\ S \end{bmatrix}, \tag{8.3}$$

where

$$\begin{aligned} P &= \alpha\beta\alpha, \\ Q &= (\alpha\beta + I)A^* - \alpha B^*, \\ R &= (\alpha\beta + I)A^*a + \alpha B^*b. \end{aligned}$$

The eigenvalues of the block matrix $M = [P, Q; U, V]$ determine the stability of rebalanced splitting.

Note 1. $P = \alpha\beta\alpha$ is the usual matrix from one step of splitting for the homogeneous system without balancing.

Note 2. In the special case that $AB = BA$ and $a = b = 0$, ordinary splitting is exact (when the substep integrations with $e^{Ah/2}$ and e^{Bh} are exact as above). Rebalanced splitting does not share this property.

Note 3. Rebalanced splitting preserves the correct steady state y_∞ for all values of h. If the step starts from $y_n = y_\infty$ and $c_n = c_\infty$, then it ends with those values (and also $y_n^+ = y_n^{++} = y_\infty$).

Note 4. Rebalanced splitting retains the second-order accuracy of Strang splitting, following the augmented representation of (4.3).

Note 5. If iteration with M is stable, we expect the solution to converge to y_∞ like $|\lambda|^n$ after n steps where λ is the eigenvalue of largest modulus.

For the block matrix M that governs the recurrence (8.3), we can compute the limits as $h \to \infty$ and $h \to 0$. Assume as before that all eigenvalues of A and B have negative real parts. Then $\alpha = e^{Ah/2}$ and $\beta = e^{Bh}$ approach zero as $h \to \infty$. The limits of A^* and B^* are $-A^{-1}$ and $-B^{-1}$ at $h = \infty$, and zero at $h = 0$. For the block matrix, both limits have *half the eigenvalues equal to* 1. The other half are zero:

$$\lim_{h\to\infty} \begin{bmatrix} P & Q \\ U & V \end{bmatrix} = \begin{bmatrix} 0 & -A^{-1} \\ 0 & I \end{bmatrix}, \tag{8.4}$$

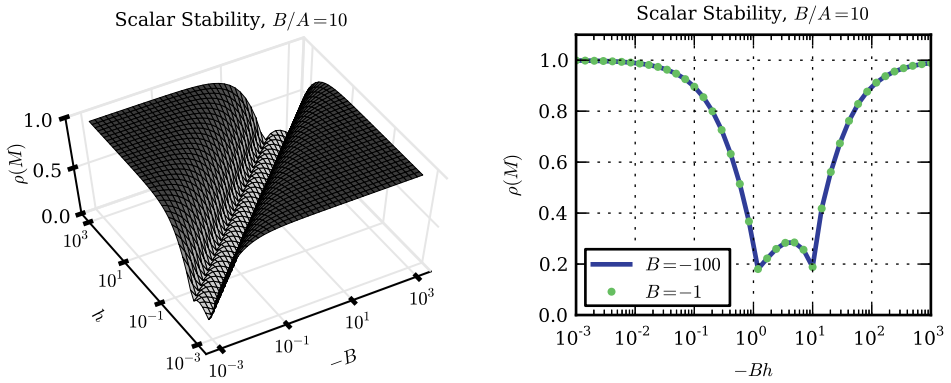

FIG. 8.1. *Maximum of the absolute value of the eigenvalues $\rho(M)$ of the 2×2 matrix $M = [P\,Q;\ U\,V]$ defined in* (8.3). *All numerical examples show a maximum less than* 1, *which points to stability in the real, scalar case. These plots suggest that $\rho(M)$ depends only on* two *parameters: B/A and Bh.*

$$\lim_{h\to 0} \begin{bmatrix} P & Q \\ U & V \end{bmatrix} = \begin{bmatrix} I & 0 \\ \frac{1}{2}(B-A) & 0 \end{bmatrix}. \tag{8.5}$$

Thus the stability condition $B/A < 3$ for simple balanced splitting (scalar case) is no longer required.

The expressions for P, Q, U, V make the eigenvalues of M difficult to analyze for finite $h > 0$. Numerical experiments, with negative numbers A and B, indicate stability. Figure 8.1 shows a typical graph of the spectral radius $\rho(M)$, which is the maximum magnitude of the eigenvalues $\lambda(M)$. This example and others suggest that rebalanced splitting is stable for all real scalars $A < 0$ and $B < 0$ and all $h > 0$. A complete proof of this conjecture has been elusive.

The next step allows 2×2 matrices A and B. We could go directly to a nonlinear problem in combustion, for which the rebalanced splitting method was created. The method is successful (section 9) for the time-dependent problem, and balancing greatly improves the computed steady state. First, however, we stay with linear analysis to see whether stability can finally break.

The matrices will have negative definite symmetric parts $\frac{1}{2}(A + A^T)$ and $\frac{1}{2}(B + B^T)$. The conventional Strang splitting remains strongly stable, as in section 3. Notice there is no control of the antisymmetric parts. In one set of experiments we steadily increased b in the following matrix A:

$$A = \begin{bmatrix} -\epsilon & b \\ -b & -\epsilon \end{bmatrix}, \qquad B = \begin{bmatrix} -1 & 0 \\ 0 & -1 \end{bmatrix}. \tag{8.6}$$

The commutator is zero and ordinary splitting is exact. However, rebalanced splitting eventually became unstable. For example, results for these matrices with the values $\epsilon = 0.01$ and $b = 100$ are shown in Figure 8.2.

It is natural to wonder about matrices for which the symmetric part is not negative definite. Consider this example with A and B nonsymmetric and with symmetric parts that have a positive eigenvalue:

$$A = \begin{bmatrix} 0.7 & -3 \\ 2 & 0.5 \end{bmatrix}, \qquad B = \begin{bmatrix} -1 & -0.2 \\ 1.1 & 0.1 \end{bmatrix}. \tag{8.7}$$

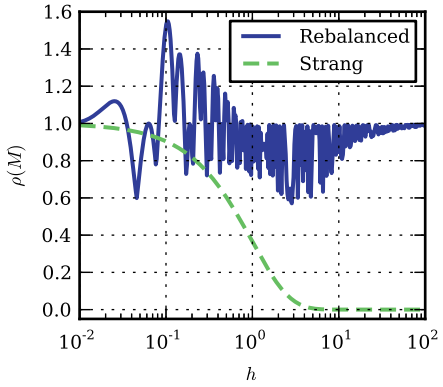

FIG. 8.2. *The symmetric parts of A and B in* (8.6) *are negative definite. Strang splitting is strongly stable ($\rho = e^{-(1+\epsilon)h}$) but rebalanced splitting is unstable ($\rho(M) > 1$) for some step sizes.*

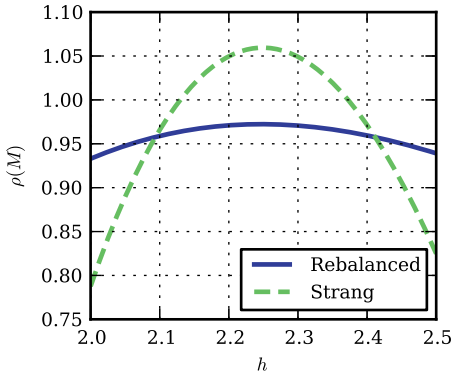

FIG. 8.3. *The symmetric part is not negative definite in example* (8.7). *For some step sizes, Strang splitting is unstable, and rebalanced splitting is stable.*

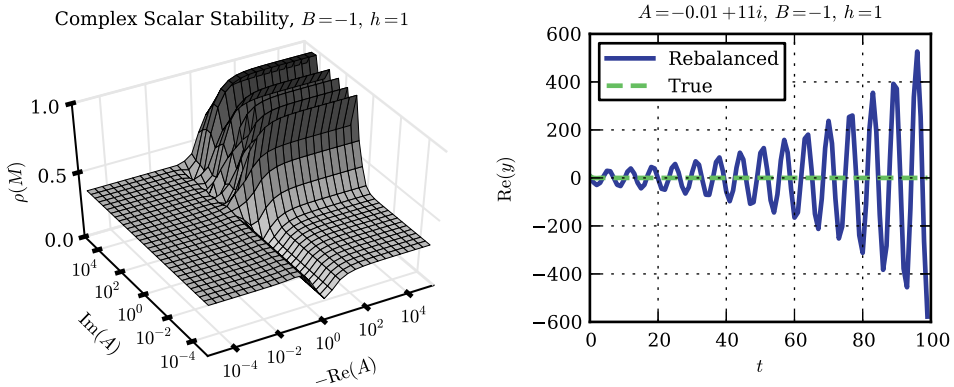

FIG. 8.4. *Here A is a complex scalar with a negative real part, and $B < 0$ is real. Left: Maximum of the absolute value of the eigenvalues of the 2×2 matrix $M = [PQ;\ UV]$ defined in* (8.3). *The maximum is ≈ 1.04 so some parameter values are unstable. Right: An example of instability. The real part of the solution shows growing oscillations.*

With this choice of A and B, for some values of h Strang splitting is unstable while rebalanced splitting is stable, as shown in Figure 8.3.

These experiments suggested a return to the scalar case, allowing *complex* scalars. Again the stability of the rebalanced splitting scheme can be broken, for example when $\mathrm{Im}(A) \approx 1000\,\mathrm{Re}(A)$ (Figure 8.4).

9. Application: Nonlinear advection–diffusion–reaction equation. Now we test the new balanced splitting methods on a significant model problem from combustion. A laminar premixed flame is stabilized in the stagnation flow produced by a pair of opposed jets. A mixture of fuel and oxidizer introduced through one jet is consumed in a chemical reaction, releasing heat which causes the reaction front to propagate into the unburned mixture. This reaction front is counteracted by the velocity of the jet, producing a quasi-steady planar flame at a particular point in the flow field. This is the steady state.

The strained flame is modeled by a system of coupled PDEs which describe the conservation of mass, momentum, energy, and chemical species [15]. With a suitable set of simplifying approximations—specifically, when the thermodynamic and transport properties of the gas are independent of composition and temperature, and all the thermal and molecular diffusivities are equal—the original equations become linearly dependent. We can then solve a scalar PDE in the surrogate variable y which varies between 0 and 1 as the mixture varies from unburned reactants at the inlet temperature to burned products at the adiabatic flame temperature. The chemical reaction can be modeled by a single-step Arrhenius rate rule for a molecular reaction, which can be written in terms of y as

$$\mathcal{R}(y) = A\,(1-y)\,e^{-E/(y-p)}, \tag{9.1}$$

where A, E, and p are constants associated with the reaction. The resulting advection–diffusion–reaction equation is then

$$\frac{\partial y}{\partial t} = -v(x)\frac{\partial y}{\partial x} + D\frac{\partial^2 y}{\partial x^2} + A\,(1-y)\,e^{-\frac{E}{y-p}}, \tag{9.2}$$

where $v(x)$ is the convective velocity and D is the diffusion coefficient. In this example, we solve (9.2) for $0 \le x \le 1$ on the interval $t = [0,1]$ with the coefficients $v(x) = -10x$, $D = 0.1$, $A = 2 \times 10^6$, $E = 8$, and $p = -0.1$. The initial condition is $y_0(x) = 0.5 \cdot (1 - \mathrm{erf}(8 \cdot (x - 0.7)))$. The boundary conditions at $x = 0$ and $x = 1$ are $y = 1$ and $y = 0$, respectively.

The equations are discretized on a uniform grid with spacing $\Delta x = 0.02$. We use a first-order upwind scheme for advection and a second-order centered difference for diffusion. The system of nonlinear ODEs is integrated using the fourth-order Runge–Kutta method with a timestep size of $h = 2 \times 10^{-4}$, which is 1/10 of the stability-limited step size $\Delta x^2/2D = 2 \times 10^{-3}$. This method is also used for integrating the split terms.

Several snapshots of the transient solution are shown in Figure 9.1. The system asymptotically approaches its steady-state solution. The solution is visually indistinguishable from the steady state for $t \ge 0.5$. If we evaluate the Jacobian matrices associated with the full system, the transport term, and the reaction term using $y_\infty(x)$, we find that all eigenvalues of the full system and the transport term have negative real parts. But the reaction term has both positive and negative eigenvalues; that substep is not strongly stable. Our earlier stability analysis does not apply. Nevertheless, splitting methods are able to produce stable solutions to this problem.

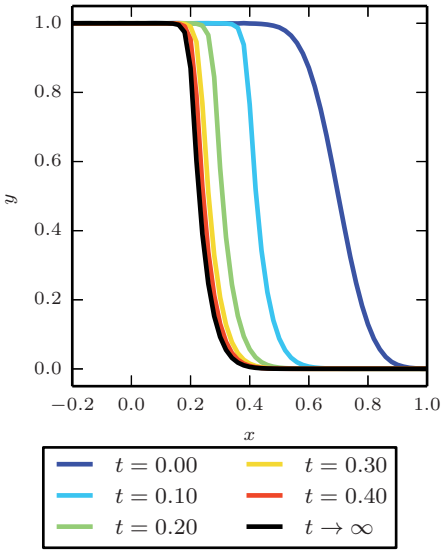

FIG. 9.1. *Transient solution to the one-dimensional reacting flow problem (see* (9.2)*).*

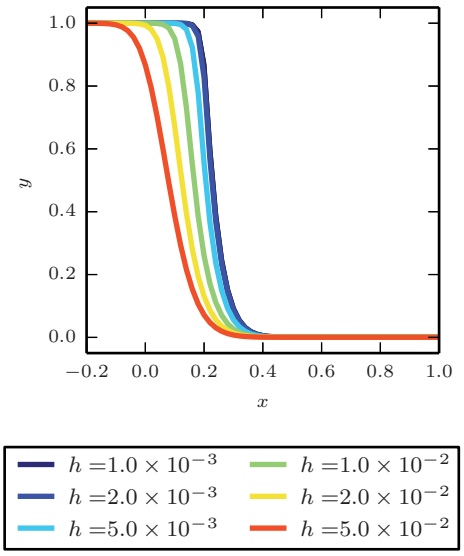

FIG. 9.2. *Steady-state solutions to the reacting flow problem obtained by Strang splitting as a function of* $h = \Delta t$.

For this example, standard second-order splitting is stable for all timestep sizes in our experiments, but it produces significant errors in both the steady-state and transient solutions. The steady-state solution obtained using Strang splitting is shown for different timesteps in Figure 9.2. The error (calculated as the 2-norm of $y - y_{\text{full}}$) in the Strang splitting solution as a function of time is shown in Figure 9.3.

The transient errors associated with simple balanced splitting are shown in Figure 9.4(a). This method is stable only for relatively small timesteps. With $h = 5 \times 10^{-3}$,

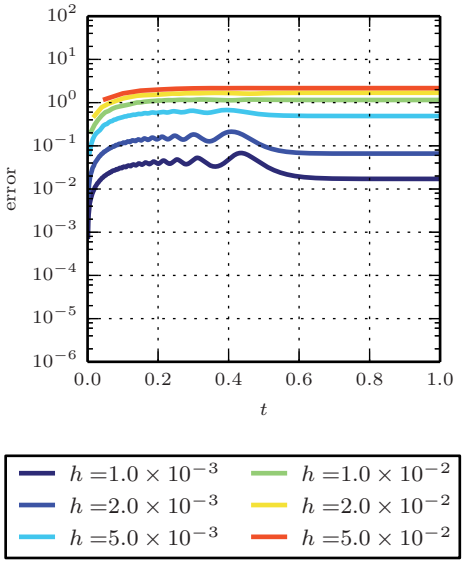

FIG. 9.3. *Error in the solution to the reacting flow problem obtained by Strang splitting as a function of timestep size.*

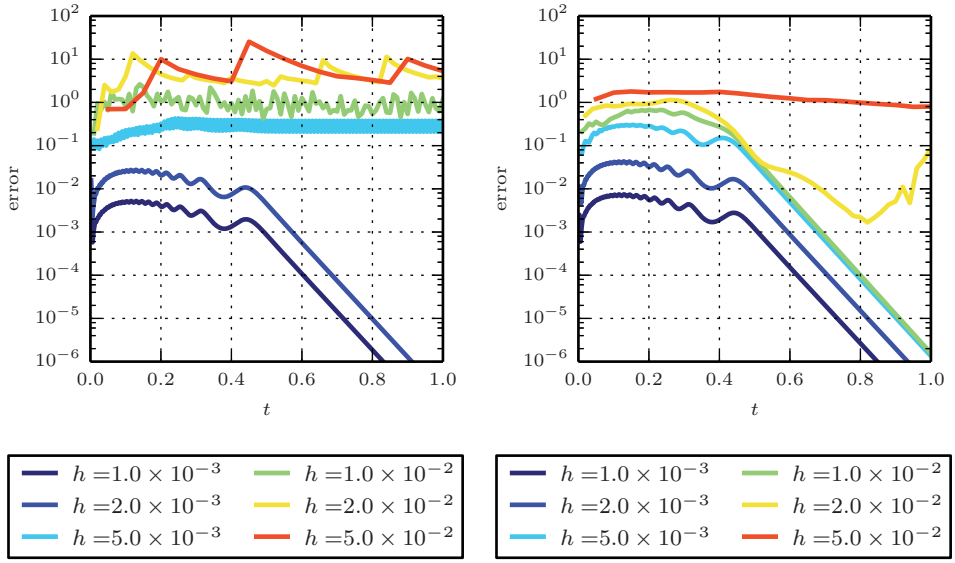

(a) *Simple balanced splitting.* (b) *Rebalanced splitting.*

FIG. 9.4. *Error in the solution to the reacting flow problem obtained by simple balanced splitting* (a) *and rebalanced splitting* (b) *as a function of* $h = \Delta t$.

the solution oscillates between two states which effectively bracket the true steady-state solution. The region where the instability manifests itself corresponds to the most negative Jacobian elements of the reaction term. A larger step size makes the method unstable.

The transient errors associated with rebalanced splitting are shown in Figure 9.4(b). Rebalanced splitting is stable for substantially larger timesteps than simple splitting, but it too becomes unstable for sufficiently large Δt. In those cases where both of the balanced methods are stable, the error associated with the simple balancing method is slightly smaller. When either balanced or rebalanced splitting is stable, the error in the transient solution is smaller than the error produced by the conventional Strang splitting method for all times. After the initial transient, the error decreases in a straight line on the log-linear scale, indicating that the method converges geometrically. The success of rebalanced splitting for this problem leads us to recommend the method, particularly in the approach to steady state.

The steady-state solution can, in principle, be obtained by solving the nonlinear algebraic system directly using Newton's method. However, in practice the strong nonlinearities prevent Newton solvers from converging in the absence of a good initial guess. Some solvers for steady-state reacting flow problems address this restriction by combining time-marching and Newton iteration [10]. In such solvers, rebalanced splitting could be used in the time-marching step to produce reasonable starting points for the Newton solver. Other implementations avoid the complexity of coupling with iterative solvers by using time-marching to obtain the steady state directly [1].

10. Application: Chemical master equation. When all species are present in high concentrations, continuum models for chemical reactions are appropriate. When some species are present in small numbers of molecules and fluctuations may be significant, a discrete, stochastic modeling framework is required. The chemical master equation (CME) provides such a framework [30]. It is based on microphysics [7], it agrees with continuum models in the limit of large numbers [16], and the CME model has become popular for single-molecule experiments and for biochemical reactions inside a cell [24, 18].

The master equation describes the evolution of the probability distribution associated with a continuous-time, discrete state Markov process [30]. Each possible state of the system x_i is a vector of nonnegative integers, where the nth component records the population of the nth species. When the jth chemical reaction occurs, the state changes from x_i to $x_i + \nu_j$, where ν_j is a stoichiometric vector of integers recording the change in the number of molecules of each species. Each reaction has a nonnegative propensity function, $\alpha_j(x_i)$, such that $\alpha_j(x_i)dt$ is approximately the probability of the reaction in the next time interval dt. The probability of state x_i evolves according to the master equation:

$$\frac{dP(x_i,t)}{dt} = \sum_j \alpha_j(x_i-\nu_j)P(x_i-\nu_j,t) - P(x_i,t)\sum_j \alpha_j(x_i). \tag{10.1}$$

If we let p be a vector with $P(x_i,t)$ as the ith component, then the master equation can be expressed as

$$p' = Mp. \tag{10.2}$$

The off-diagonals of M are $m_{kl} \geq 0$, the propensity for a reaction that takes state l to state k. The diagonal terms produce zero column sums. If $p(0)$ is the initial probability distribution, then $p(t)$ is a probability vector for all time.

When M is finite and bounded, the solution may be computed as a matrix exponential [25]. Solving the CME directly is usually challenging because the matrix M may be very large. The CME is often approached by a Monte Carlo stochastic simulation algorithm [7]. And direct solution methods for the CME have recently made progress [22].

In many applications it is natural to split M into different parts arising from different types of reactions, so that the CME is $p' = Ap + Bp$ (where $M = A + B$). Jahnke and Altintan describe splitting and an error estimate for the stochastic simulation algorithm [14]. Strang splitting has also been adopted for the direct solution of the master equation [21], and for reaction-diffusion master equations [6, 4]. Applications of splitting can involve reactions with very different time scales, so that A and B may represent fast and slow reactions, though usually a type of quasi-steady-state approximation is also applied [3, 5, 20].

The stationary probability distribution of the CME will often be computed numerically by large-scale linear eigenvector solvers, or by Monte Carlo, but in some cases it may be computed by long time integration of the master equation. We now demonstrate that errors in the steady state can be corrected by balanced splitting.

Two examples of master equations arising in biochemical kinetics are now described. We consider a natural splitting based on reaction types. In all examples $[A, B] \neq 0$, so there is some splitting error. Symmetric Strang splitting is a very good choice for Michaelis–Menten enzyme kinetics. Balanced splitting offers advantages when the goal is to capture the stationary distribution of the Goldbeter–Koshland switch.

Example. Michaelis–Menten enzyme kinetics [31] involves the conversion of a substrate S into a product P, catalyzed by an enzyme E and proceeding via a complex intermediate C:

$$S + E \leftrightarrow C \leftrightarrow P + E.$$

It is natural to split this into $S + E \leftrightarrow C$ as a master equation with matrix A, and $C \leftrightarrow P + E$ with matrix B. In general, there is a splitting error because $[A, B] \neq 0$. If we begin precisely at the stationary distribution, p_∞, there is zero splitting error because it happens that $Ap_\infty = Bp_\infty = 0$. Balanced splitting has no advantage over ordinary splitting.

Example. The Goldbeter–Koshland switch [9] involves two enzymes E and F that catalyze opposing reactions:

$$\begin{aligned} &S + E \leftrightarrow C \rightarrow P + E, \\ &P + F \leftrightarrow D \rightarrow S + F. \end{aligned} \tag{10.3}$$

When E is a kinase and F is a phosphatase, this models the first of three stages of the mitogen activated protein kinase cascade [12]. In this example, $Ap_\infty \neq 0$ and $Bp_\infty \neq 0$. We expect that symmetric Strang splitting will not exactly preserve the stationary distribution but that balanced splitting will. To test this, we choose an example that is small enough to compute exponentials in full. Figure 10.1 confirms that for the Goldbeter–Koshland switch, balanced splitting is more accurate than Strang splitting for computing the stationary distribution. During the initial transient, however, Strang splitting is more accurate than balanced splitting. The behavior of the error in this example suggests that a good approach is to combine Strang splitting with balanced splitting: begin integrating with Strang splitting, and then for large t, as steady state is approached, change to balanced splitting.

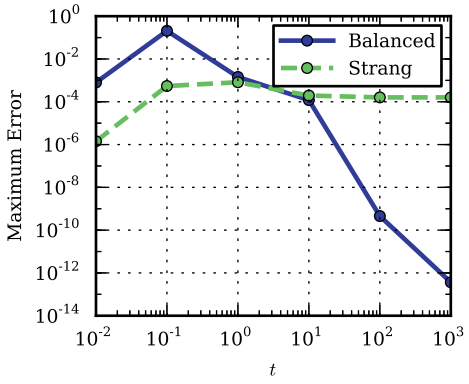

FIG. 10.1. *Comparison of symmetric Strang splitting with simple balanced splitting for the CME associated with the Goldbeter–Koshland switch* (10.3). *For large t, as the stationary distribution is approached, balanced splitting is more accurate than Strang splitting. Parameters: Initial state is* $[S\ E\ C\ P\ F\ D] = [10,\ 10,\ 0,\ 0,\ 10,\ 0]$, *and the rate constants are* 1 *for the reversible reactions, and* 0.1 *for the irreversible reactions.*

Stability. As a Markov process, $p(0)$ and $p(t)$ are probability vectors: $p_i(t) \geq 0$ (componentwise) and $1 = 1^T p(t) = \sum p_i(t)$, where 1^T is a row vector of ones. Evaluating $p(t) = e^{tM} p(0)$ with exact exponentials is unconditionally stable. It is natural to split based on reaction types, and in this case the split operators A and B separately describe Markov processes. Thus Strang splitting preserves key properties of the exact equation for each split operator, separately, and it is unconditionally stable. In contrast, balanced splitting does not ensure positivity, nor that $||p(t)||_1 = 1$, and the method may be unstable for some step sizes.

However, the following conservation property is respected by balanced splitting. The master equation matrix M satisfies $1^T M = 0$. Hence $1^T p(t) = 1^T p(0) = 1$ is constant. When splitting maintains $1^T B = 0$ and $1^T A = 0$, the balancing vector, $c = (1/2)(B - A)p$ satisfies $1^T c = 0$. Then $1^T p(t) = 1^T p(0) = 1$ also for balanced splitting. In summary, balanced splitting applied to the CME is often more accurate than conventional splitting for long time integration, and for capturing the stationary distribution.

11. Conclusions. The new rebalanced splitting method proposed here converges to the true steady state. We expect it will usually be more accurate than conventional second-order splitting because its approximate split steps involve smaller excursions away from the true trajectory than those of conventional splitting. We believe it will be beneficial in many practical applications, since often the fast modes are close to steady state during most of a computed trajectory. If numerical instabilities arise, which sometimes happens, one would be well advised to fall back on the conventional second-order "Strang" splitting method.

Appendix A. Steady-state error of Strang splitting. Consider a variant of (1.2) where $r = a = -b$. Then (1.2) is homogeneous but the split equations are not:

$$y' = (Ay + r) + (By - r)\,. \tag{A.1}$$

The steady-state solution to this equation is $y_\infty = 0$. For simplicity, we introduce the following notation:

$$\alpha = e^{Ah/2}, \quad \beta = e^{Bh}, \quad A^* = (\alpha - I)A^{-1}, \quad B^* = (\beta - I)B^{-1}. \tag{A.2}$$

Integrating this equation using Strang splitting starting at y_n and using a timestep of h, we obtain the following:

$$y_n^{+} = \alpha y_n + A^* a, \tag{A.3}$$

$$y_n^{++} = \beta\alpha y_n + \beta A^* r - B^* r, \tag{A.4}$$

$$y_{n+1} = \alpha\beta\alpha y_n - \alpha B^* r + (\alpha\beta + I)\, A^* r. \tag{A.5}$$

The steady-state solution of the Strang splitting method can be found by solving the linear system obtained by substituting $y_n = y_{n+1} = y_\infty$ into (A.5):

$$(I - \alpha\beta\alpha)\, y_\infty = [(\alpha\beta + I)\, A^* - \alpha B^*]\, r. \tag{A.6}$$

We can now show that $y_\infty = \mathcal{O}(h^2)$ by writing the Taylor series for each term in the preceding equation:

$$I - \alpha\beta\alpha = (A + B)h + (A^2 + B^2 + BA + AB)\frac{h^2}{2} + \mathcal{O}(h^3) = \mathcal{O}(h), \tag{A.7}$$

$$(\alpha\beta + I)\, A^* - \alpha B^* = \left(\frac{A^2}{24} + \frac{B^2}{12} + \frac{BA}{8}\right) h^3 + \mathcal{O}(h^4) = \mathcal{O}(h^3). \tag{A.8}$$

With $r = \mathcal{O}(1)$, the leading orders of the terms in (A.6), show that

$$\mathcal{O}(h) \cdot y_\infty = \mathcal{O}(h^3) \cdot \mathcal{O}(1). \tag{A.9}$$

Thus the splitting error in y_∞ is $\mathcal{O}(h^2)$.

REFERENCES

[1] H. M. Altay, K. S. Kedia, R. L. Speth, and A. F. Ghoniem, *Two-dimensional simulations of steady perforated-plate stabilized premixed flames*, Combust. Theor. Model., 14 (2010), pp. 125–154.

[2] S. Blanes, F. Casas, P. Chartier, and A. Murua, *Optimized high-order splitting methods for some classes of parabolic equations*, Math. Comp., 82 (2013), pp. 1559–1576.

[3] Y. Cao, D. T. Gillespie, and L. R. Petzold, *The slow-scale stochastic simulation algorithm*, J. Chem. Phys., 122 (2005), 014116.

[4] B. Drawert, M. J. Lawson, L. Petzold, and M. Khammash, *The diffusive finite state projection algorithm for efficient simulation of the stochastic reaction-diffusion master equation*, J. Chem. Phys., 132 (2010), 074101.

[5] W. E, D. Liu, and E. Vanden-Eijnden, *Nested stochastic simulation algorithm for chemical kinetic systems with disparate rates*, J. Chem. Phys., 123 (2005), 194107.

[6] S. Engblom, L. Ferm, A. Hellander, and P. Lötstedt, *Simulation of stochastic reaction-diffusion processes on unstructured meshes*, SIAM J. Sci. Comput., 31 (2009), pp. 1774–1797.

[7] D. Gillespie, *Markov Processes: An Introduction for Physical Scientists*, Academic Press, Boston, 1992.

[8] S. K. Godunov, *Finite difference methods for numerical computation of discontinuous solutions of the equations of fluid dynamics*, Mat. Sb., 47 (1959), pp. 271–295.

[9] A. Goldbeter and D. E. Koshland, Jr., *An amplified sensitivity arising from covalent modification in biological systems*, Proc. Natl. Acad. Sci. USA, 78 (1981), pp. 6840–6844.

[10] J. F. Grcar, R. J. Kee, M. D. Smooke, and J. A. Miller, *A hybrid Newton/time-integration procedure for the solution of steady, laminar, one-dimensional premixed flames*, P. Combust. Inst., 21 (1986), pp. 1773–1782.

[11] E. Hairer, C. Lubich, and G. Wanner, *Geometric Numerical Integration: Structure-Preserving Algorithms for Ordinary Differential Equations*, Springer-Verlag, Berlin, 2006.

[12] C. Y. Huang and J. E. Ferrell, *Ultrasensitivity in the mitogen-activated protein kinase cascade*, Proc. Natl. Acad. Sci. USA, 93 (1996), pp. 10078–10083.
[13] W. Hundsdorfer and J. G. Verwer, *Numerical Solution of Time-Dependent Advection-Diffusion-Reaction Equations*, Springer-Verlag, Berlin, 2003.
[14] T. Jahnke and D. Altintan, *Efficient simulation of discrete stochastic reaction systems with a splitting method*, BIT, 50 (2010), pp. 797–822.
[15] R. J. Kee, M. E. Coltrin, and P. Glarborg, *Chemically Reacting Flow: Theory and Practice*, John Wiley & Sons, Hoboken, NJ, 2003.
[16] T. G. Kurtz, *The relationship between stochastic and deterministic models of chemical reactions*, J. Chem. Phys., 57 (1972), pp. 2976–2978.
[17] J. Lee and B. Fornberg, *A split step approach for the* 3*-D Maxwell's equations*, J. Comput. Appl. Math., 158 (2003), pp. 485–505.
[18] G.-W. Li and X. S. Xie, *Central dogma at the single-molecule level in living cells*, Nature, 475 (2011), pp. 308–315.
[19] W.-C. Lo, M. Wang, L. Chen, and Q. Nie, *A robust and efficient method for steady state patterns in reaction diffusion systems*, J. Comput. Phys., 231 (2012), pp. 5062–5077.
[20] S. MacNamara, A. M. Bersani, K. Burrage, and R. B. Sidje, *Stochastic chemical kinetics and the total quasi-steady-state assumption: Application to the stochastic simulation algorithm and chemical master equation*, J. Chem. Phys., 129 (2008), 095105.
[21] S. MacNamara, K. Burrage, and R. B. Sidje, *Application of the Strang splitting to the chemical master equation for simulating biochemical kinetics*, International J. Computational Science, 2 (2008), pp. 402–421.
[22] S. MacNamara, K. Burrage, and R. B. Sidje, *Multiscale modeling of chemical kinetics via the master equation*, Multiscale Model. Simul., 6 (2008), pp. 1146–1168.
[23] G. I. Marchuk, *Some application of splitting-up methods to the solution of mathematical physics problems*, Appl. Math., 13 (1968), pp. 103–132.
[24] H. H. McAdams and A. Arkin, *Stochastic mechanisms in gene expression*, Proc. Natl. Acad. Sci. USA, 94 (1997), pp. 814–819.
[25] C. Moler and C. Van Loan, *Nineteen dubious ways to compute the exponential of a matrix,* 25 *years later*, SIAM Rev., 45 (2003), pp. 3–49.
[26] D. W. Peaceman and H. H. Rachford, Jr., *The numerical solution of parabolic and elliptic differential equations*, J. Soc. Indust. Appl. Math., 3 (1955), pp. 28–41.
[27] D. L. Ropp and J. N. Shadid, *Stability of operator splitting methods for systems with indefinite operators: Reaction-diffusion systems*, J. Comput. Phys., 203 (2005), pp. 449–466.
[28] D. A. Schwer, P. Lu, W. H. Green Jr., and V. Semião, *A consistent-splitting approach to computing stiff steady-state reacting flows with adaptive chemistry*, Combust. Theory Model., 7 (2003), pp. 383–399.
[29] G. Strang, *On the construction and comparison of difference schemes*, SIAM J. Numer. Anal., 5 (1968), pp. 506–517.
[30] N. G. van Kampen, *Stochastic Processes in Physics and Chemistry*, Elsevier, Amsterdam, 2001.
[31] N. G. Walter, *Michaelis-Menten is dead, long live Michaelis-Menten!* Nat. Chem. Biol., 2 (2006), pp. 66–67.
[32] H. Yoshida, *Construction of higher order symplectic integrators*, Phys. Lett. A, 150 (1990), pp. 262–268.